J Forensic Sci, March 2008, Vol. 53, No. 2
doi: 10.1111/j.1556-4029.2007.00644.x
Available online at: www.blackwell-synergy.com

John Coumbaros,[1] *Ph.D.; John Denman,*[2,3] *B.Sc. (Hons.); K. Paul Kirkbride,*[4] *Ph.D.; G. Stewart Walker,*[2] *Ph.D.; and William Skinner,*[3] *Ph.D.*

An Investigation into the Spatial Elemental Distribution Within a Pane of Glass by Time of Flight Secondary Ion Mass Spectrometry

ABSTRACT: Advances in the technology employed for the manufacture of glass have resulted in a final glass product with little variability in terms of its physical and optical properties. For example, the refractive index of Australian float glass tends to lie between 1.5189 and 1.5194. It has therefore become necessary to complement physical and optical methods for forensic glass comparison with instrumental elemental analyses. In a previous study, time-of-flight secondary ion mass spectrometry has been shown to offer potential for the analysis of glass particles as small as a few tens of microns across. In this study, the three-dimensional homogeneity of a sheet of float glass is described, and consequences for forensic elemental analysis of glass particles of such size are explored. Variation in Si, Ca, Mg, and Na levels immediately under the nonfloat surface was observed, with the variance accompanied by a decrease in refractive index.

KEYWORDS: forensic science, trace evidence, glass, time of flight secondary ion mass spectrometry, refractive index, elemental analysis

Because of the ubiquitous occurrence of glass, it is one of the most frequently encountered types of evidence in forensic science (1), with the majority of cases involving float window glass from incidents such as burglaries. In forensic glass examinations, a routine method involves comparison of refractive index (RI) of control and recovered samples. The RI measurement technique is rapid and inexpensive, performed on instruments such as Foster & Freeman's (Worcestershire, UK) glass refractive index measurement (GRIM) apparatus (2,3). However, advances in glass technology and tighter controls on raw materials and processes used in the manufacture of glass have resulted in a narrowing of the RI distribution of sheet glass (1,4,5). As a consequence, it is now not unusual for float glass from different origins to have indistinguishable refractive indices.

Hence, numerous forensic laboratories now employ elemental analysis techniques to perform glass comparisons (6). In a number of studies, it was found that elemental analysis techniques could successfully be employed in conjunction with RI to discriminate between samples, where RI data alone could not. Such studies utilized spectrophotometric techniques including SEM-EDX (7–9), ED-XRF (8,10), μ-XRF (8), ICP-AES (10–12), and mass spectrometric techniques including ICP-MS (8,13,14), LA-ICP-MS (15), and time-of-flight secondary ion mass spectrometry (TOF-SIMS).

The TOF-SIMS is an elemental analysis technique that was recently shown by us to have potential in the forensic analysis of gunshot residues (16,17) and glass. Our initial work on the analysis of glass involved the elemental distribution between different glass samples, but we did not establish to what extent the elemental composition varied within a given sample, such as a sheet of window glass. Trejos and Almirall (18), using LA-ICP-MS, have demonstrated that samples as small as 200 ng have an elemental composition representative of the entire pane. However, as TOF-SIMS analysis involves depth penetration of at least two orders of magnitude less than is used in LA-ICP-MS, elemental heterogeneity might still be a concern if the former technique is used.

The variation of RI across (i.e., along *X* and *Y* axes) and through the thickness (i.e., along the *Z* axis) of sheet glass is well documented (7,19–25). It has been established that most of the RI variation in the *Z* axis arises as a result of structural stress in the sheet. In the case of toughened glass, in which structural stress is deliberately induced through rapid freezing of the surface of glass heated above its stress point, the change in RI (or ΔRI) between surface and bulk glass is quite marked. In glass that has not gone through the tempering process, such as float window glass, ΔRI is much smaller. To be not misled by the affects of residual structural stress, forensic glass comparison can include an annealing step that relieves it. It is evident, however, that an additional phenomenon contributes to a change in RI along the *Z* axis in glass manufactured by the float process. It has been found (22–24) that the RI of the tin contact surface of float glass is higher than that of the bulk, whereas the nonfloat surface exhibits an RI lower than the bulk. As "thermal history" should result in both surfaces having a positive ΔRI compared with the bulk, that effect alone would not appear to account for the phenomenon at the nonfloat surface at least. In the manufacture of float glass, one surface of the glass (the float surface) is in contact with molten tin while the opposite surface (the nonfloat surface) is exposed to a hot reducing N_2/H_2 atmosphere within the tin float bath (26,27). It has been established that the incorporation of tin into the float surface causes an increase of RI (28–36), while depletion of species such as Fe, Na_2O, CaO, and SO_3 in the nonfloat surface results in a locally higher concentration of

[1]Defence Science and Technology Organisation, Human Protection and Performance Division, 506 Lorimer Street, Fishermans Bend, Vic. 3207, Australia.
[2]School of Chemistry, Physics and Earth Sciences, Flinders University, South Australia, GPO Box 2100, Adelaide 5001, South Australia.
[3]Ian Wark Research Institute, Mawson Lakes Boulevard, Mawson Lakes, South Australia.
[4]National Institute of Forensic Science, PO Box 13075, Law Courts Post Office, Vic. 8010, Australia.

Received 30 Oct. 2005; and in revised form 1 Sept. 2006; accepted 22 Oct. 2006.

Si, and therefore a decrease in the RI (28,31,35). In these studies, etching solvents (HF) were used so as to erode the glass surface so that the sub-surface glass might be analyzed. It was not indicated whether the procedure caused the preferential leaching of any elements (28,31).

It has been established that during the act of breaking a window, a large proportion of particles deposited onto the person breaking the window originate from the surface closest to them (37–41). Furthermore, in case work, it is not unusual to encounter particles containing less than 200 ng of glass. If techniques such as SIMS are to be exploited to reduce the analytical domain of glass analysis, then the extent to which the elemental levels at that domain represent the levels in the bulk must be established.

This article describes an investigation into the elemental variation within a pane of float glass, particularly within the nonfloat surface regions where it is known that the RI differs significantly from the bulk and there is some literature evidence to suggest that trace element concentrations vary as well.

Methods

Glass Samples

Clear window float glass (nontempered) 100 × 100 cm, 3 mm thick, was purchased from Marion Glass (Adelaide, South Australia). According to the supplier, this is a typical sheet of float glass supplied for window glass in Adelaide. The sample was cut in half to obtain two sheets of 100 cm × ~50 cm. One of these sheets was sectioned further using a glasscutter so as to obtain samples suitable for RI and TOF-SIMS analysis. A schematic of the sectioned sheet is illustrated in Fig. 1. The float surface of the sectioned samples was identified using UV-irradiation at 254 nm.

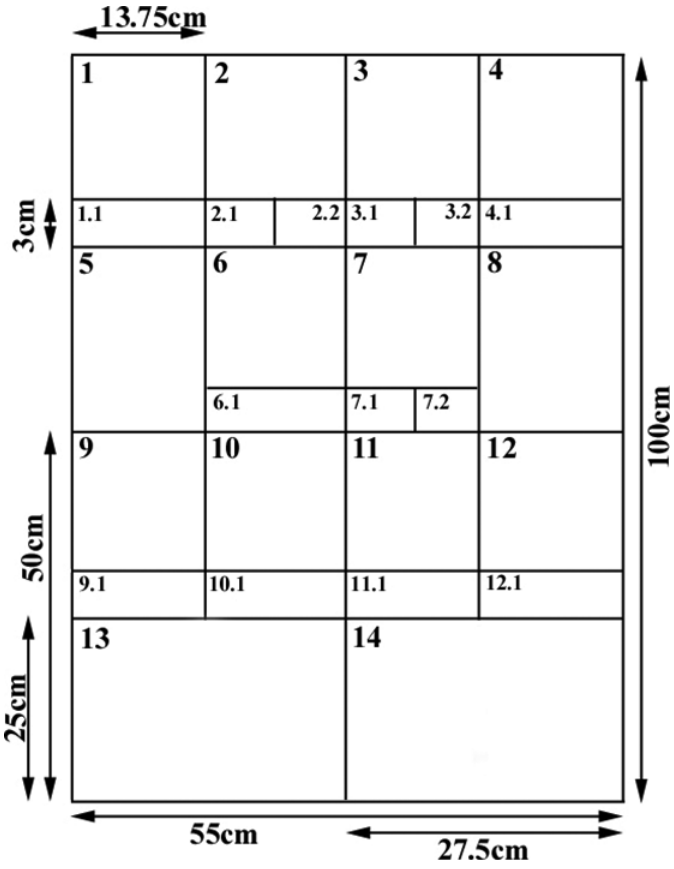

FIG. 1—*Schematic illustrating the sectioning of the float glass sample.*

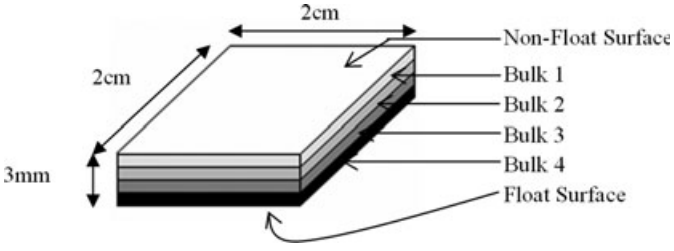

FIG. 2—*Layering as a function of glass thickness.*

Glass Sampling for RI Analysis

Glass samples of 2 × 2 cm were obtained from five locations (1.1, 4.1, 6.1, 9.1, 12.1) across the sheet of glass as shown in Fig. 1. Each of these samples was crushed to obtain fragments across the 3 mm width of the glass sheet. This was performed using a modification of a method of Newton et al. (41):

- Different colored permanent-inks were used to mark four layers through the thickness of the glass, as well as to color the float and nonfloat surface (Fig. 2), a total of six samples through the 3 mm thickness.
- The colored edges were broken and crushed, and fragments collected. The fragments were carefully separated into groups according to color.
- Large fragments and those containing more than one color were crushed further.
- The surface of the chip was struck obliquely and the thin surface layer fragments produced were collected.
- The sample fragments, now separated into six groups based on color, were placed in vials into which acetone was added. The vials were agitated to help remove the ink, drained, and left to stand for residual acetone to evaporate.

The method outlined above enabled the collection of fragments from both surfaces, as well as from four layers through the bulk. Upon recovery of the fragments they were prepared for GRIM (technique outlined below) by placing them onto a GRIM microscope slide, immersing in precalibrated silicone oil, and covering with a cover slip.

Glass Sampling for TOF-SIMS Analysis

Pieces of glass of 1 × 1 cm were obtained from sections 2.1, 3.2, 7.1, 10.1, and 11.1 (refer to Fig. 1), selected to be in as close as possible proximity to the samples obtained for RI analysis. The samples were mounted on 12 mm diameter SEM stubs with carbon adhesive, nonfloat side up. Prior to TOF-SIMS analysis, the surface of the glass samples was wiped with acetone to remove any extraneous contamination. A further two 1 × 1 cm samples were obtained from section 2.1, selected to assess the elemental variation as a function of depth. These samples were mounted in resin for easier handling, nonfloat side up and abraded using silicon carbide sanding disks, thus allowing the removal of 0.5 mm (labeled as Sample 2.1 [2.5 mm]) and 0.8 mm (labeled as Sample 2.1 [2.2 mm]) of material from the nonfloat surface. The glass samples were recovered from the resin by dissolving the resin in dichloromethane, and mounted on 12 mm diameter SEM stubs with carbon adhesive, with the freshly etched surface up permost.

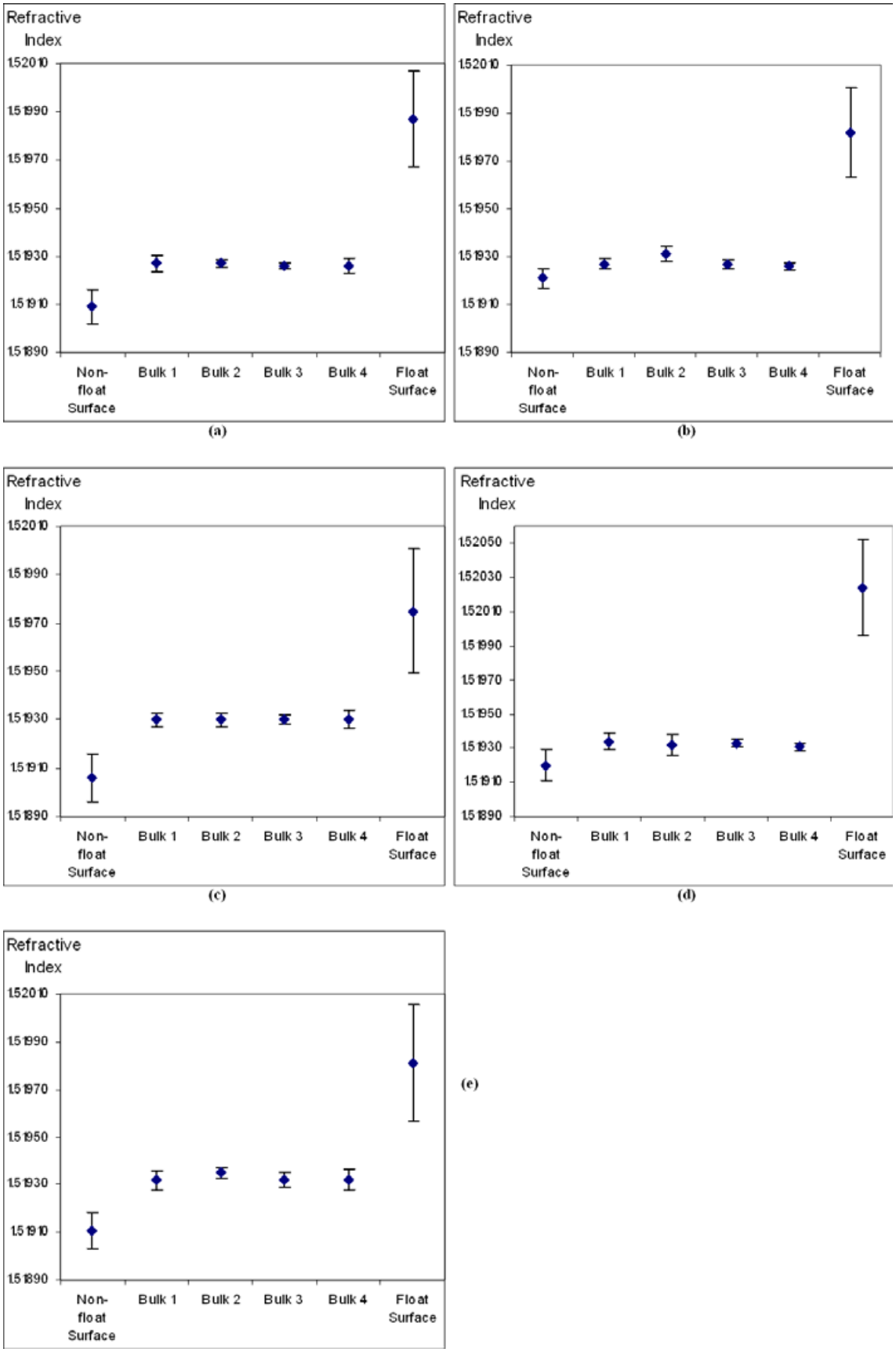

FIG. 3—*Variation of refractive index (RI) through the thickness (99% confidence interval) measured for glass fragments (a) 1.1; (b) 4.1; (c) 6.1; (d) 9.1; (e) 12.1.*

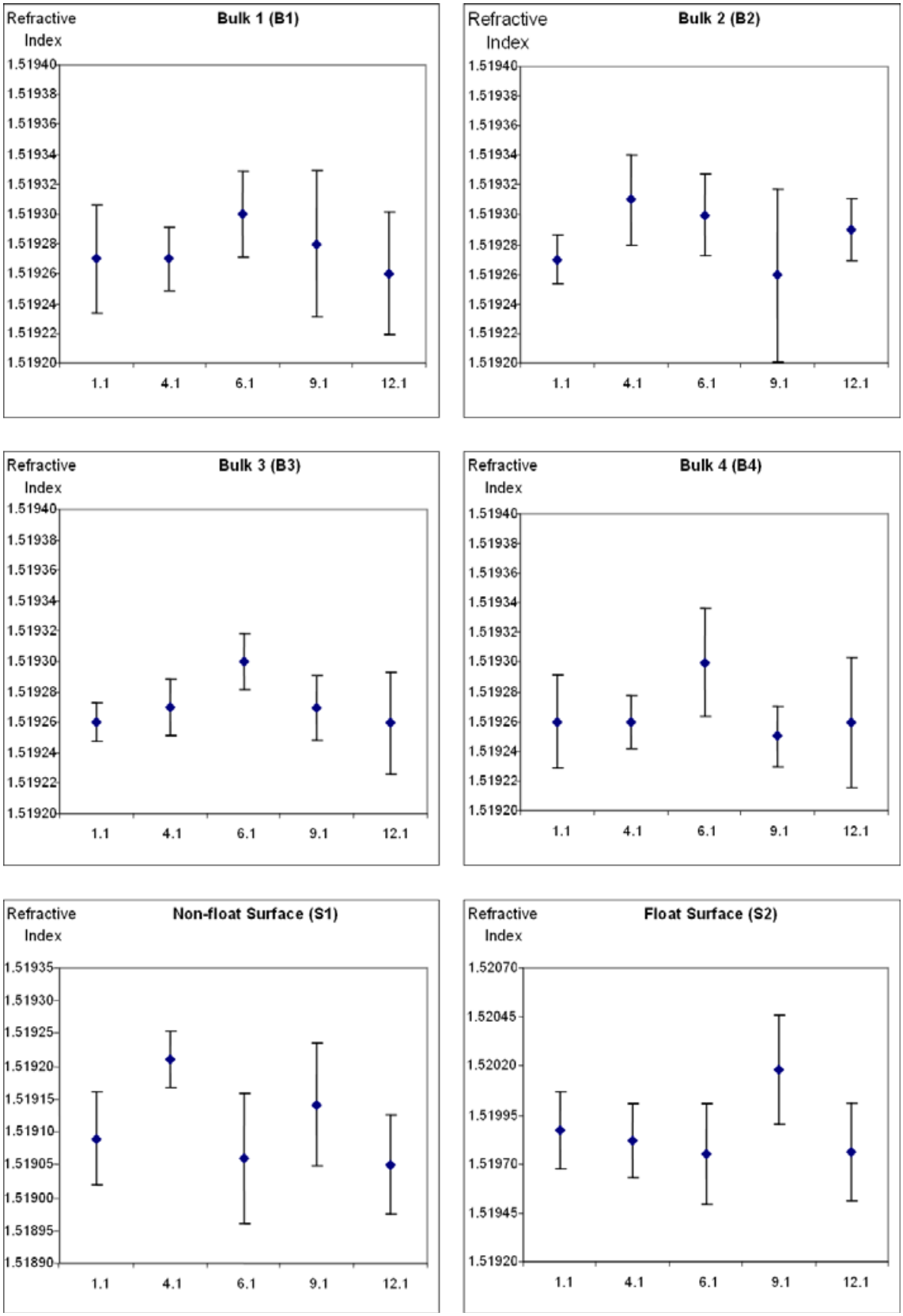

FIG. 4—*Refractive index measurements across the sheet of glass (99% confidence interval).*

Instrumental Parameters

Refractive Index—A Foster and Freeman (Worcestershire, UK) GRIM3 GRIM apparatus was used for the measurement of RI. The apparatus consists of a Leica DMLB2 phase contrast microscope with a Mettler Toledo FP82HT Hotstage and a monochrome CCD video camera, interfaced to a desktop computer. Analysis was performed using the heat–cool cycle set at 5°C/min. A minimum of

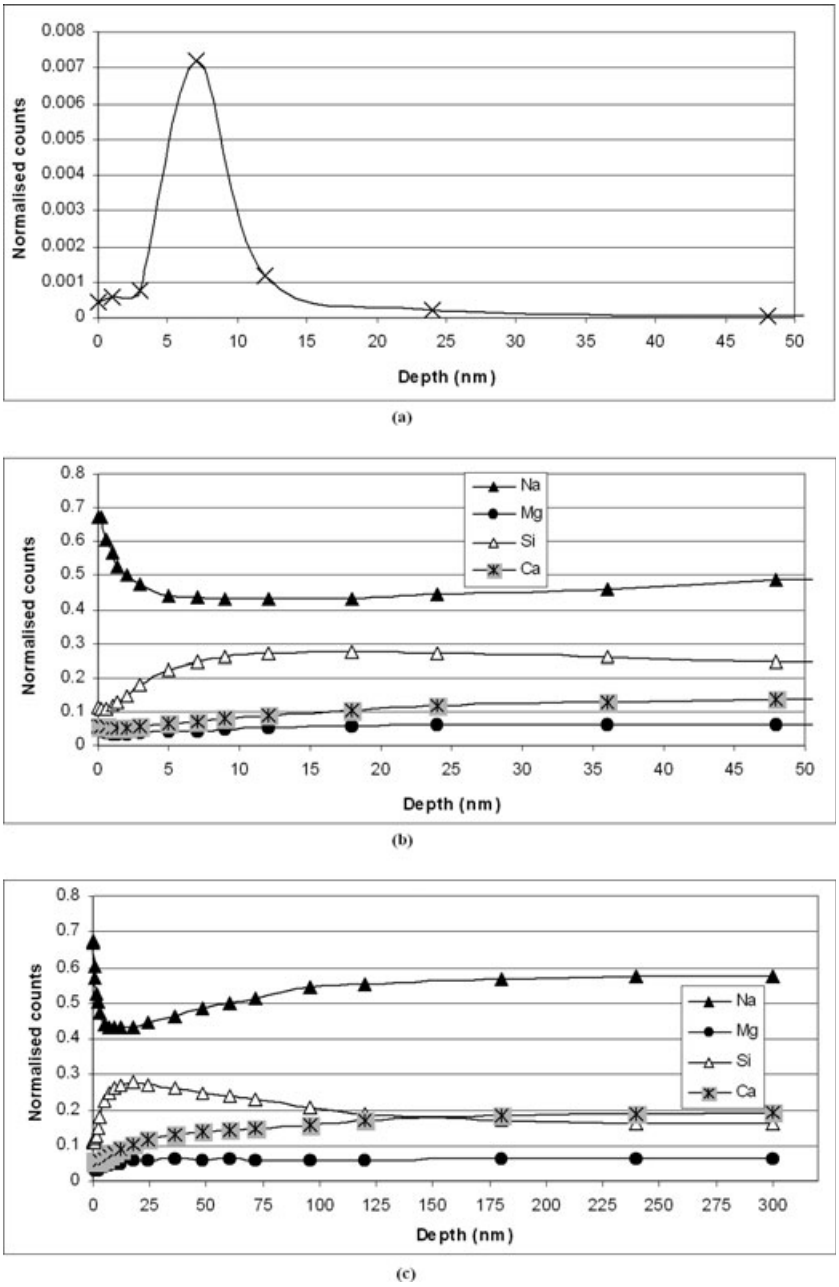

FIG. 5—*(a) Tin depth profile on nonfloat surface; (b) and (c) silicon, sodium, calcium, and magnesium depth profile on nonfloat surface.*

10 replicate analyses were performed per sample (error bars on figures depicting RI measurements are indicative of twice the standard deviation of the replicate measurements). Analysis of a "daily" standard (known RI) was performed for calibration purposes, and to compensate for any instrumental drift between measurements performed on different days.

TOF-SIMS—A Physical Electronics, Inc. (MN, USA) Model 2100 PHI TRIFT II^{TM} TOF-SIMS equipped with a pulsed liquid metal $^{69}Ga^{+}$ primary ion gun (LMIG) was used for the analysis. The LMIG was operated at 15 kV energy, 600 pA beam current, and 18 nsec pulse length. The LMIG was also operated in continuous (DC) beam mode for controlled periods, allowing the removal of sequential layers of the surface, while in pulsed beam mode a mass spectrum was acquired from each exposed layer, thus acquiring a depth profile of the sample.

Results and Discussion

Variation of RI Through the Glass Thickness

Refractive index measurements were performed on a minimum of 10 fragments originating from each layer. The data for each sample are illustrated in Fig. 3. Statistical *t*-tests, performed at a 99% confidence interval, provided evidence that there was no significant difference in the RI data of the bulk fragments, with the exception of sample fragment 4.1, where the *t*-test suggested that a difference existed between the RI of Bulk 2 and the other bulk fragments.

The nonfloat surface exhibited a RI lower than that of the bulk, while the RI of the float-surface was significantly higher than the bulk. For both surfaces, the variance in RI data was greater than that exhibited for the bulk glass, with the variance in the float surface greater than that for the nonfloat surface. These findings are consistent with literature reports (22–24).

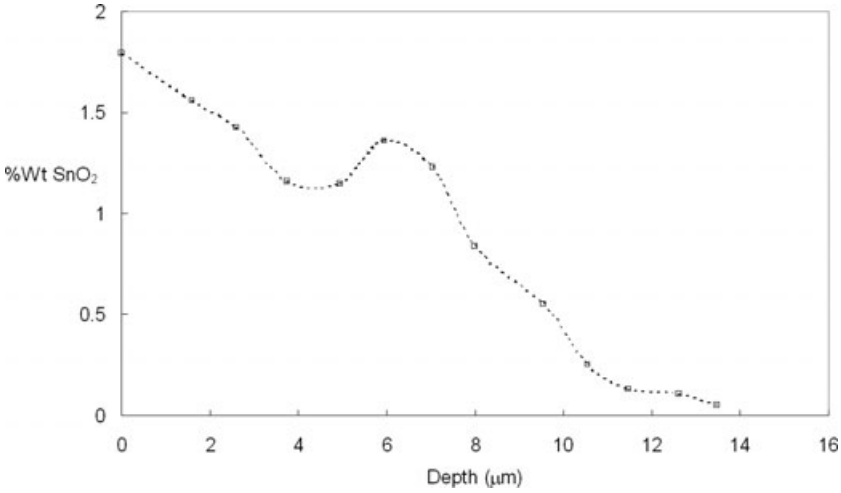

FIG. 6—*Tin profile on float surface (adapted from Sieger [28]).*

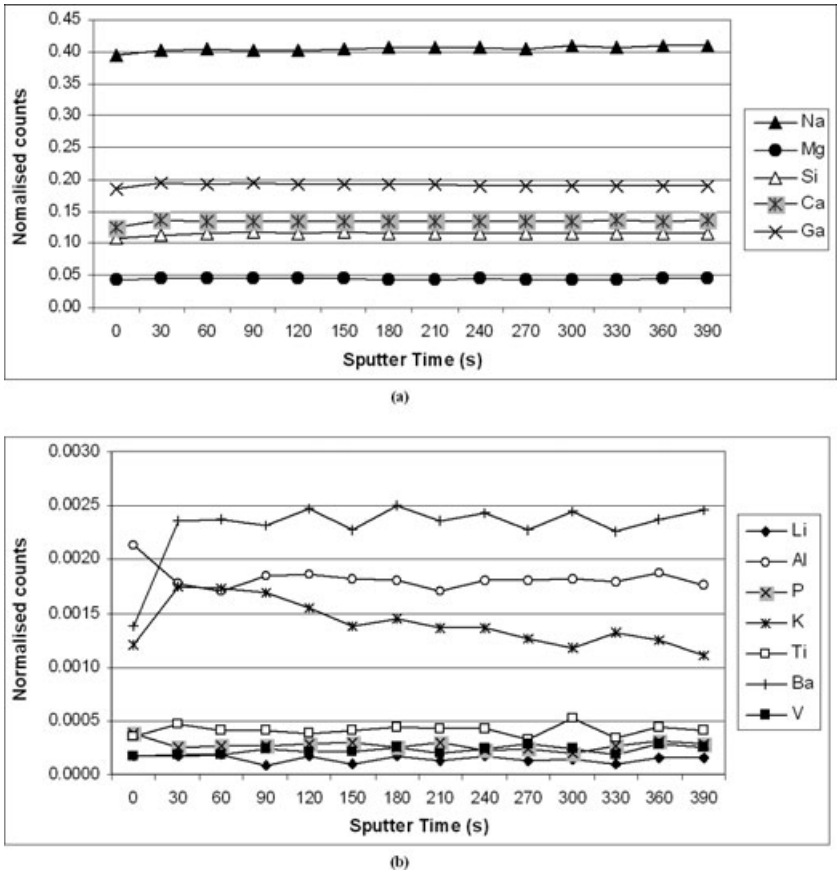

FIG. 7—*Elemental depth profiles (a) bulk elements and (b) trace elements.*

Variation of RI Across the Sheet of Float Glass

The RI measured across the pane is illustrated in Fig. 4; no significant difference in RI is apparent.

Elemental Homogeneity of Float Glass as a Function of Depth

The elements Li, B, Na, Mg, Al, Si, P, K, Ca, Ti, V, Cr, Ni, Co, Cu, Sn, and Ba were selected for monitoring based on recommendations in the literature and preliminary work (7). Depth profiles however were limited to 14 elements due to software limitations; the elements Li, B, Na, Mg, Al, Si, P, K, Ca, Ti, Ba, V, Ga (primary ion-beam), and Sn were selected.

Figure 5*a* represents the tin depth profile of a nonfloat surface fragment taken from region 7.2 (refer to Fig. 1) in the pane. The *x*-axis in Fig. 5 has been converted to depth by assuming an average sputter rate of 0.2 nm/sec (Skinner, 2002 personal communication). Furthermore, the elemental data have been normalized with reference to total counts.

Clearly there is a regionally high level of tin in the glass 4–11 nm from the nonfloat surface. This profile resembles the "tin hump" found in the analysis of glass directly under float surfaces, which is reported elsewhere (28,34,43,44) and reproduced in Fig. 6.

Figure 5*b* shows the depth profiles for other elements over the same region. The depletion of tin with depth appears to be correlated with depletion in sodium, magnesium, and calcium and enrichment in silicon. It should be noted that the depth profiles represent an elemental response and do not represent absolute concentration. Further to this it became evident that a sputter period of 1500 sec, equivalent to a depth of approximately 300 nm into the nonfloat surface, is required for the elements to provide a steady response (Fig. 5*c*). Therefore, for any subsequent analyses of nonfloat surfaces, a minimum sputter period of 1500 sec was used prior to any comparison of the elemental data.

Repetitive depth profiles acquired after the initial 1500 sec sputter period (Fig. 7) confirmed that the observed surface heterogeneity disappears and a steady "homogeneous" response is observed for bulk and trace elements. Figure 7 therefore suggests that the profiled elements are homogeneous from a depth of *c*. 300–380 nm. The only exception was potassium, which throughout this TOF-SIMS investigation appeared to be an unstable element in the glass matrix.

To assess elemental variance at greater depths within the bulk, cross-sections were examined. Analyses were performed in three regions—*c*. 400 μm from the nonfloat surface, in the edge-center, and *c*. 400 μm from the float surface. Comparison of the data is presented in Fig. 8.

Statistical *t*-tests indicate that a small difference exists in the concentrations of sodium and magnesium between the three analyses. All other bulk elements and all trace elements fall within the error range (two times standard deviation) and there is no significant difference as determined by the *t*-tests.

Elemental Variation Across the Pane of Glass

Analyses were performed on the nonfloat surface, and data comparison was performed on data obtained after an initial 1500 sec sputter period to eliminate any contribution from tin diffusion and any subsequent elemental variation. Data were obtained from the analysis of the glass fragments 2.1, 7.1, and 11.1 (refer to Methods section). Comparison of the data is presented in Fig. 9. Error bars are represented as two times the standard deviation.

The data suggest no significant difference for most of the profiled elements. Exceptions to this were phosphorus, vanadium, and nickel with respect to Sample 2.1 Analysis 1, for which a second

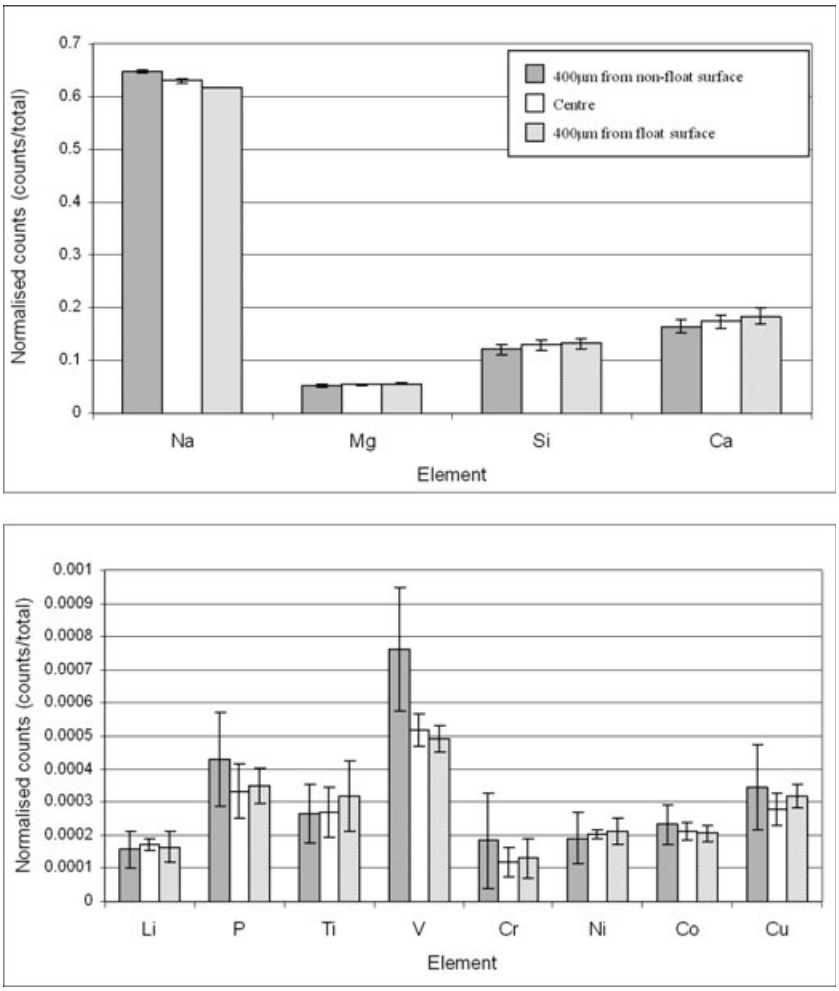

FIG. 8—*Elemental distribution as a function of depth.*

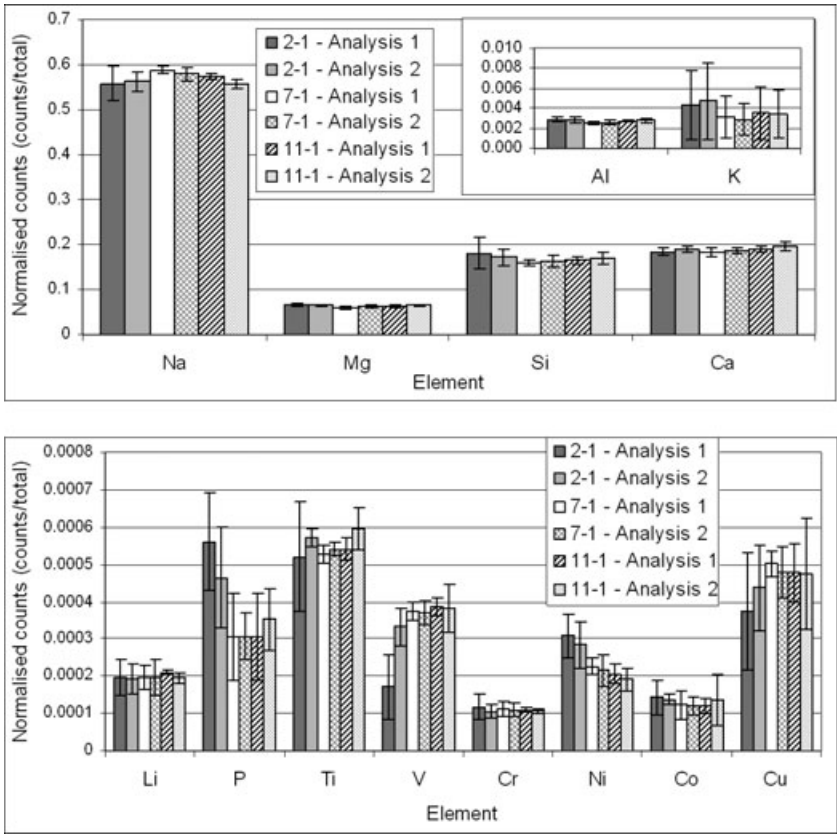

FIG. 9—*Elemental variation across the pane of the glass.*

analysis of the same sample indicated that this may have been an outlier.

Relationship Between Surface RI Measurements and Elemental Distribution

Results obtained by TOF-SIMS indicate an "enrichment" of Si and depletion of Na and Ca and possibly Mg in glass nonfloat surfaces. This confirms earlier work that relied upon acid etching as a means of depth profiling the nonfloat surface and therefore would appear to eliminate the possibility that leaching was responsible for the observed depletion of Na, Ca, and Mg (28–36).

Conclusion

Results presented here confirm that the RI of both the float and nonfloat surfaces differs significantly from the RI of the bulk. These results support the practice of avoiding float surface fragments, which are easily distinguished, when measuring RI. This work also indicates that the analysis of nonfloat surface fragments is also not straightforward as their RI and elemental composition is not representative of the bulk. This is of significance because nonfloat surface fragments are not as easily recognized as float surface fragments. The work reported here confirms other studies that have concluded that there is no significant variation in RI and elemental composition across the pane with reference to fragments recovered from the bulk (i.e., by avoiding surface fragments).

The variation in elemental composition demonstrated in this article is not a concern if analytical conditions are such that the glass surface is sampled to a depth beyond a few microns, for example under the conditions reported by Trejos and Almirall (18). However, where analytical techniques such as SIMS are used, which operate to a depth measured in tens and hundreds of nanometers, the glass examiner must take care so as to avoid Type 1 errors. Either the surface under examination should be subjected to erosion until bulk glass is exposed, or surfaces originating from the bulk must be chosen.

Work in our laboratory is continuing in an effort to describe the extent of tin diffusion in the float surface and its impact upon elemental composition.

Acknowledgments

The authors would like to acknowledge the assistance of Des Phillips from Forensic Science South Australia, Angus Netting while he was at the Ian Wark Research Institute, University of South Australia, and Dr. Jose Almirall of the International Forensic Research Institute at Florida International University who provided invaluable input and stimulated important discussions. This project was partially financed through Flinders University Early Career Research Grant to G. Stewart Walker and an Honours Research Grant to John Denman and G. Stewart Walker.

References

1. Buscaglia J. Elemental analysis of small glass fragments in forensic science. Anal Chim Acta 1994;288:17–24.
2. Foster & Freeman. GRIM3—Glass refractive index measurement. Available at http://www.fosterfreeman.co.uk/grim3.html (accessed 5th March 2003).
3. Locke J, Underhill M. Automatic refractive index measurement of glass particles. Forensic Sci Int 1985;27:247–60.

4. Koons RD, Buscaglia J. Distribution of refractive index values in sheet glasses. Forensic Sci Comm 2001;3(1):1–5.
5. Almirall J. Elemental analysis of glass fragments. In: Caddy B, editor. Forensic examination of glass and paint. London: Taylor and Francis, 2001;65–83.
6. Collaborative Testing Services Inc. Test No. 01-548 Glass analysis. Available at http://www.colaborativetesting.com/reports/2148_web.pdf 2001.
7. Andrasko J, Maehly AC. The discrimination between samples of window glass by combining physical and chemical techniques. J Forensic Sci 1978;23(2):250–62.
8. Becker S, Gunaratnam L, Kicks T, Stoecklein W, Warman G. The differentiation of float glass using refractive index and elemental analysis: comparisons of techniques. Probl Forensic Sci 2001;47:80–92.
9. Reeve V, Mathiesen J, Fong W. Elemental analysis by energy dispersive X-ray: a significant factor in the forensic analysis of glass. J Forensic Sci 1976;21(2):291–306.
10. Koons RD, Peters CA, Rebbert PS. Comparison of refractive index, energy dispersive X-ray fluorescence and inductively coupled plasma atomic emission spectrometry for forensic characterization of sheet glass fragments. J Anal Atom Spectrom 1991;6:451–6.
11. Almirall JR, Cole MD, Gettinby G, Furton KG. Discrimination of glass sources using elemental composition and refractive index: development of predictive models. Sci Justice 1998;38(2):93–100.
12. Koons RD, Buscaglia J. The forensic significance of glass composition and refractive index measurement. J Forensic Sci 1999;44(3):496–503.
13. Parouchais T, Warner IM, Palmer LT, Kobus H. The analysis of small glass fragments using inductively coupled plasma mass spectrometry. J Forensic Sci 1996;41(3):351–60.
14. Suzuki Y, Sugita R, Suzuki S, Marumo Y. Forensic discrimination of bottle glass by refractive index measurement and analysis of trace elements with ICP-MS. Anal Sci 2000;16:1195–8.
15. Bakowska E, Cerven J, Schultz B, Kristiansen D. Quantitative analysis of glass samples by LA-ICP-MS. Available at http://www.chem.agilent.com/temp/rad61C10/00034252.pdf (accessed 5th March 2003).
16. Coumbaros J, Kirkbride KP, Klass G, Skinner W. Characterisation of 0.22 caliber rimfire gunshot residues by time-of-flight secondary ion mass spectrometry (TOF-SIMS): a preliminary study. Forensic Sci Int 2001;119:72–81.
17. Collins P, Coumbaros J, Horsley G, Lynch B, Kirkbride KP, Skinner W, et al. Glass-containing gunshot residue particles: a new type of highly characteristic particle? J Forensic Sci 2003;48(3):538–53.
18. Trejos T, Almirall JR. Sampling strategies for the analysis of glass fragments by LA-ICP-MS Part I. Micro-homogeneity study of glass and its application to the interpretation of forensic evidence. Talanta 2005;67:388–95.
19. Dabbs MDG, Pearson EF. The variation in refractive index and density across two sheets of window glass. J Forensic Sci Soc 1970;10:139–48.
20. Bennett RL, Kim ND, Curran JM, Coulson SA, Newton AWN. Spatial variation of refractive index in a pane of float glass. Sci Justice 2003;43(2):71–6.
21. Locke J, Hayes CA. Refractive index variations across glass objects and the influence of annealing. Forensic Sci Int 1984;26:147–57.
22. Underhill M. Multiple refractive index in float glass. J Forensic Sci Soc 1980;20:169.
23. Zoro JA, Locke J, Day RS, Badmus O, Perryman AC. An investigation of refractive index anomalies at the surfaces of glass objects and windows. Forensic Sci Int 1988;39:127–41.
24. Davies MM, Dudley RJ, Smalldon KW. An investigation of bulk and surface refractive indices for flat window glasses, patterned window glasses and windscreen glasses. Forensic Sci Int 1980;16:125–37.
25. Newton AWN, Kitto L, Buckleton JS. A study of the performance and utility of annealing in forensic glass analysis. Forensic Sci Int 2005;155:119–25.
26. Pilkington LAB. The float glass process. Proc R Soc Lond A 1969;314:1–25.
27. Bloomfield LA. Windows and glass. In: Bloomfield LA, editor. How things work: the physics of everyday life. Virginia: John Wiley and Sons, 2001;16(16.2):1–10. Available at http://www.htw.wiley.com/htw/ch16/ch16_2/windows_and_glass.pdf.
28. Sieger JS. Chemical characteristics of float glass surfaces. J Non-Cryst Solids 1975;19:213–20.
29. Colombin L, Jelli A, Riga J, Pireaux JJ, Verbist J. Penetration depth of tin in float glass. J Non-Cryst Solids 1977;24(2):253–8.
30. Colombin L, Charlier H, Jelli A, Debras G, Verbist J. Penetration of tin in the bottom surface of float glass: a synthesis. J Non-Cryst Solids 1980;38/39(2):551–6.
31. Baitinger WE, French PW, Swarts EL. Characterization of tin in the bottom surface of float glass by ellipsometry and XPS. J Non-Cryst Solids 1980;38/39(2):749–54.
32. Dugnoille B, Rase I, Virlet O. Tin depth profile in surface layers of float glass. Proc Soc Photo-Opt Inst 1994;2253(2):1313–22.
33. Townsend PD, Can N, Chandler PJ, Farmery BW, Lopez-Heredero R, Peto A, et al. Comparisons of tin depth profile analyses in float glass. J Non-Cryst Solids 1998;223:73–85.
34. Hayashi Y, Matsumoto K, Kudo M. The diffusion mechanism of tin into glass governed by redox reactions during the float process. J Non-Cryst Solids 2001;282:188–96.
35. Lamouroux F, Can N, Townsend PD, Farmery BW, Hole DE. Ion beam analysis of float glass surface composition. J Non-Cryst Solids 1997;212:232–42.
36. Williams KFE, Johnson CE, Nikolov O, Thomas MF, Johnson JA, Greengrass J. Characterization of tin at the surface of float glass. J Non-Cryst Solids 1998;242:183–8.
37. Nelson DF, Revell BC. Backward fragmentation from breaking glass. J Forensic Sci Soc 1967;7:58–63.
38. Zoro JA. Observations on the backward fragmentation of float glass. Forensic Sci Int 1983;22:213–9.
39. Luce RJW, Buckle JL, McInnis I. A study on the backward fragmentation of window glass and the transfer of glass fragments to individual's clothing. J Can Soc Forensic Sci 1991;24:79–89.
40. Locke J, Scranage JK. Breaking of flat glass—part 3: surface particles from windows. Forensic Sci Int 1992;57:73–80.
41. Newton AWN, Curran JM, Triggs CM, Buckleton JS. The consequences of potentially differing distributions of the refractive indices of glass fragments from control and recovered sources. Forensic Sci Int 2004;140:185–93.
42. Frischat GH, Müller-Fildebrandt C, Moseler D, Heide G. On the origin of the tin hump in several float glasses. J Non-Cryst Solids 2001;283:246–9.
43. Wang TJ, Zhang H, Zhang G, Yuan T. Computer modelling of satellite peak in tin profile of float glass. J Non-Cryst Solids 2000;271:126–36.
44. Williams KFE, Johnson CE, Greengrass J, Tilley BP, Gelder D, Johnson JA. Tin oxidation state, depth profiles of Sn^{2+} and Sn^{4+} and oxygen diffusivity in float glass by Mössbauer spectroscopy. J Non-Cryst Solids 1997;211:164–72.
45. Hickman DA, Harbottle G, Sayre EV. The selection of the best elemental variables for the classification of glass samples. Forensic Sci Int 1983;23:189–212.

Additional information and reprint requests:
John Coumbaros, Ph.D.
Human Protection and Performance Division
Defence Science and Technology Organisation
506 Lorimer Street
Fishermans Bend 3207
Vic. 3207
Australia